The Potency of Alkaloid Derivates as Anti-Breast Cancer Candidates: In Silico Study

Sedin Renadi¹, Anindita Tri Kusuma Pratita¹, Richa Mardianingrum² dan Ruswanto Ruswanto¹*

¹Faculty of Pharmacy, Universitas Bakti Tunas Husada, Jl. Cilolohan No. 36, Tasikmalaya, 46115, Indonesia
²Faculty of Pharmacy, Universitas Perjuangan, Jl. PETA No. 177, Tasikmalaya, 46115, Indonesia

Corresponding author: ruswanto@universitas-bth.ac.id

Abstract

Breast cancer is the most frequent malignancy in women worldwide. One of the target receptors for the treatment of breast cancer are estrogen, progesterone, and HER2 receptors. An alternative treatment using natural ingredients has been developed, one of which is alkaloid compounds. This study aims to determine the activity of alkaloid compounds as anti-breast cancer agents through an in-silico method. Virtual screening (AutoDock Vina), molecular docking (AutoDock Tools), molecular dynamics (Desmond), scanning Lipinski's rule of five, as well as pharmacokinetic and toxicity parameters, were performed. The results of virtual screening, molecular docking, and molecular dynamics show that the compounds daurisoline, solasodine, and sambutoxin have stable interactions with the HER2 receptor, with the lowest values of RMSD (Root Mean Square Deviation) and RMSF (Root Mean Square Fluctuation) compared to other compounds. Based on the results of the study conducted, it was shown that daurisoline, solasodine, and sambutoxin were predicted to be used as anti-HER2 candidates for the treatment of breast cancer.

**Keywords**: Alkaloids; breast cancer; molecular dynamics; molecular tethering; virtual screening

1. INTRODUCTION

Breast cancer in women has already surpassed lung cancer as the top cause of cancer incidence globally in 2020, accounting for an expected 2.3 million new cases, or 11.7% of all cancer cases. The number of cases of death from breast cancer is 685 thousand in the world. Breast cancer ranks first in the most diagnosed cases in women (24.5%), and in cases of death it also ranks first in women (15.5%). The incidence rate of breast cancer far exceeds that of other cancers in developed countries (55.9 per 100,000) and developing countries (29.7 per 100,000). 1 in 4 incidences of cancer in women are caused by breast cancer and 1 in 6 cases causes death. Most countries in the world place breast cancer as the first order for incidence (159 out of 185 countries) and death (110 out of 185 countries) (Sung et al., 2021).

Breast cancer cells differ from normal cells in that they overexpress certain receptors. Receptor pathway modulation is an interesting therapeutic strategy in breast cancer treatment. In addition, the literature shows that the number of cases of breast cancer with positive estrogen receptors is increasing. The HER2 receptor, a subtype of the Epidermal Growth Factor Receptor (EGFR) family, is also responsible for the development of breast cancer along with the progesterone receptor. According to recent reports, resistance to drugs targeting the estrogen receptor in breast cancer, such as tamoxifen, is increasing. Therefore, it is important to identify alternative receptors to target breast cancer (Devarajan et al., 2019).

Cancer has several therapeutic options, with the fundamental method of therapy being the elimination and/or death of carcinogenic cells in order to stop cancer cell proliferation. Small molecule chemotherapy, surgery, and radiation were once the cornerstones of cancer treatment. Chemotherapy has been acknowledged as one of the tactics for battling malignant cells and tissues since the beginning of cancer treatment.
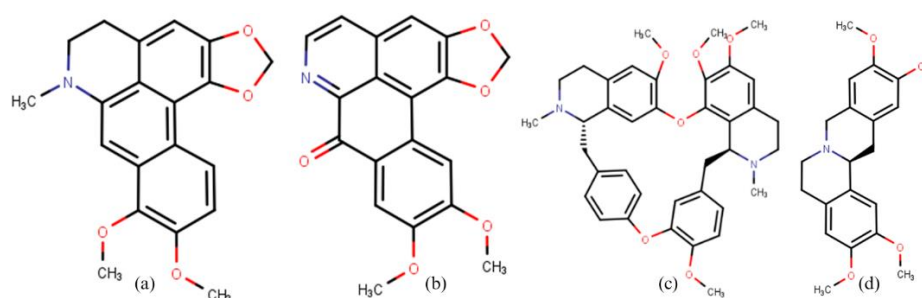
Figure 1. Structure of (a) dehydrocrebanine, (b) dicentrinone (c) tetrandrine and (d) Corytenchine

Chemotherapy's fundamental idea is to destroy cancer cells by using drugs that can impede the susceptible processes connected with cell proliferation (Islam et al., 2020). However, chemotherapy has certain undesirable side effects, such as baldness, biliousness, discomfort, and emesis (Islam et al., 2020). Based on this, several alternative therapies have been developed, including the use of natural substances with anticancer properties, such as alkaloids.

Alkaloids are a vast category of plant secondary metabolites with several therapeutic applications, one of which is as an anticancer agent. Alkaloids have anti-inflammatory effects and have demonstrated an impact on neurodegenerative disorders or Central Nervous System (CNS) diseases, along with antiviral and antimicrobial/bacterial properties (Rampogu et al., 2022). Several types of isoquinoline alkaloids, such as aporphine (dehydrocrebanine), oxoaporphine (dicentrinone and liriodenine), bisbenzylisoquinoline (tetrandrine), protoberberine (Corytenchine), benzophenanthridine (acetonyldihydrosanguinarine), and lycorine, show stronger anticancer activity than other alkaloids (Qing et al., 2017). A few examples of the alkaloid structure given in **Figure 1**. Several vegetable alkaloids have anticancer activity at micromolar or nanomolar concentrations, and their mechanisms of action are complicated and vary among the alkaloids. For example, berberine inhibited cell motility in triple-negative breast cancer cells by downregulating the transforming growth factor ß-1. When these alkaloids are combined, their anticancer efficacy against diverse cancer cell lines impacts cell growth, cell cycle, cell invasion, angiogenesis, metastasis, autophagy, and death (Tilaoui et al., 2021).

Based on the above studies regarding the anticancer activity of alkaloid compounds of various types of plants, an in silico study of alkaloid compounds as candidates for breast anticancer drugs has been carried out. From the research that has been done, it is predicted that the alkaloid compounds have stable interactions on several cancer receptors, giving a better value to parameters of lipinski drug similarity as well as pharmacokinetic and toxicity profiles, so that an increase in cancer treatment is obtained when compared to tamoxifen.

2. MATERIALS AND METHODS
Tools and materials

The tools used for this research consist of software and hardware. The software used is AutoDockTools-version 1.5.7 for molecular docking, Desmond with an academic license (D.E. Shaw Research, New York) for molecular dynamic, Discovery Studio Visualizer 2021 Client from Biovia version 21.1.0.20298 for visualize molecular docking result and preparing native ligand and protein, MarvinSketch from Chemaxon version 5.2.5.1 for test compound ligands and positive control drug compound preparation, Pymol version 2.5.4 from Schrodinger used for preparing molecular docking result for molecular dynamic, and Molegro Molecular Viewer (MMV) version 2019.7 for separating native ligand and protein. In addition, web server based software includes Protein Data Bank (PDB), Protein Structure Analysis and Verification SAVES, PubChem, PDBsum, Small-molecule pharmacokinetics prediction pkCSM, and Lipinski's Rule of Five. As for the hardware used, it is a laptop with Intel®Core™ i3-3217U CPU @ 1.80 GHz (4 cores), 10 GB DDR3 RAM, Windows 10 64-Bit operating system and a PC with Intel®Xeon(R) CPU E5-267 v2 @ 2.70 GHz (24 Core), NVIDIA GeForce RTX 3060, 7.7 GB RAM, and the Linux Ubuntu 18.04.5 LTS operating system.

The materials used in this study were taken from the PubChem compound database

and from the literature (Ruswanto et al., 2022) in the form of 370 alkaloid-derived compounds as well as three breast cancer receptors, namely the progesterone receptor (PDB ID: 1ZUC) (Zhang et al., 2005), estrogen (PDB ID: 5W9C) (Maximov et al., 2018), and HER2 (PDB ID: 7PCD) (Wilding et al., 2022).

Target Receptor Identification

The receptors were selected following the parameter criteria in the Ramachandran Plot, namely having disallowed regions values of less than 0.8% which can be seen when the PDB receptor code is entered on the website http://www.ebi.ac.uk/pdbsum/ (Laskowski et al., 1997, 2018), as well as profile checking, target receptor ERRAT analysis by entering the PDB code of each receptor on the website https://saves.mbi.ucla.edu/ (Colovos & Yeates, 1993). The ERRAT quality value is expressed in the form of a percentage of a percentage which if the value is less than 95% then it is considered rejected *(Dutta* et al., 2018; Tran et al., 2015).

Receptor Preparation

Breast cancer receptors were selected from a protein data bank with the website address http://www.rcsb.org/, then downloaded in .pdb format. Next, the water molecule and conformer are removed, followed by separating the receptor from its native ligand using the Molegro Molecular View application, then preparing the receptor and the ligand by adding hydrogen and cargo using the Discovery Studio 2021 Client application and finally saving in the .pdb format (Mardianingrum et al., 2021; Raval & Ganatra, 2022).

Ligand Preparation

The test compounds that are ligands are downloaded from the pubchem website and stored in 2D .sdf format, then converted to .mol2 format. After that, the preparation of the ligand was carried out in two stages. First, the ligands were cleaned in 2D format, protonated at the same pH as blood pH, namely 7.4 and stored in .mrv format. Second, the energy of the ligand is minimized by performing the ligand conformation using the MMFF94 (Merck Molecular Force Field) parameter (Halgren, 1999) as many as 10 conformations and results with the lowest energy stored in .pdb format. The two ligand preparation processes were carried out using the MarvinSketch software (Ruswanto et al., 2021).

Molecular Docking

This approach was validated by re-docking the native ligand with the previously separated active site of the receptor. Each receptor is made of a grid box with sizes and coordinates adjusted to their native ligands. The result is the RMSD (Root Mean Square Deviation), which is represented in angstroms (Å). If the RMSD value of ≤ 2 Å is reached, the validation of molecular docking is pronounced valid. The application to be used is AutoDock Tools (Ruswanto et al., 2022). The grid box size for each receptor is not significantly varied, the receptors (PDB: 1ZUC) and (PDB: 5W9C) have the same size, namely 40 x 40 x 40 Å respectively for x, y and z, while for the grid box size (PDB: 7PCD) has 40 x 44 x 40 Å. The grid box center for each receptor is different. For 1ZUC, the grid box dimensions are 27.746, -7.72, and 8.992 for x, y and z, respectively. For 5W9C and 7PCD, the grid box dimensions are 15.044, -10.616, and -26.4 respectively; as well as 8,413, -8,996, and -13,532.

The docking of the test compounds was carried out in two stages. First, a virtual screening was carried out using Autodock Vina (Trott & Olson, 2009), 20 modes for each ligand. The findings were then ranked based on the magnitude of the binding energy, and the 5 compounds with the lowest bond energy values for each receptor were chosen. The second stage involves docking the best chemical molecules with the same target protein as the native ligand using the AutoDockTools program and the Lamarckian GA algorithm, with each docking consisting of 150 runs. This process yields the value of the free bond energy or ΔG in kcal/mol and the value of the inhibition constant (KI) (Ruswanto et al., 2022).

The depiction of the binding findings can express the ligand's interaction with the receptor in 2D and 3D formats. In the result, the ligand-receptor conformations with the lowest free binding energies are determined, and complexes in the form of.pdb files are preserved. Visualization was carried out using Discovery Studio software (Ruswanto et al., 2022). Apart from using Discovery Studio, visualization also uses the Pymol software to see the position of the ligand against the receptor for each of the best running results.

Molecular Dynamic

Molecular dynamics was run using software namely Desmond (Schrodinger, LLC, New York, NY, USA) (Research, 2019). The stability of the best alkaloid derived compounds with each receptor was examined using molecular dynamics with one selected receptor and the best alkaloid derived compounds from the findings of molecular docking using Desmond. Molecular dynamics was carried out using TIP3P (Transferable Intermolecular Potential 3-Point) water modeling because it has no influence on the thermodynamic features of the solutes, such as the structure of thermodynamically stable conformers, but it dramatically decreases the barriers between these states, accelerating the kinetics and thereby increasing sampling in the simulations (Florová et al., 2010; Jorgensen et al., 1983) and 0.15 M NaCl to resemble physiological ionic concentrations. Energy minimization is carried out for 100 ps. The Nose-Hoover and Martyna-Tobias-Klein algorithms were used to keep all MD systems at 300 K and pressure at 1.01325 bar for 100 ns, using an orthorhombic box with buffer dimensions of 10 Å x 10 Å x 10 Å and an ensemble NPT (Ruswanto et al., 2022).

Ligand-Based Drug Similarity Screening (Drug Scan)

The best compounds that had gone through the molecular docking and molecular dynamics phases were subjected to drug scan examination. This investigation is performed to determine if a chemical compound with pharmacological or biological activity possesses chemical and physical qualities that will allow it to be used as an orally active medicine for humans (Lipinski's Rule of Five) using the website http://www.scfbio-iitd.res.in/software/drugdesign/lipinski.jsp (Jayaram et al., 2012; Lipinski, 2004).

According to Lipinski's Rule of Five, all alkaloid derivative compounds with a lower free energy value than native ligands were screened for medicines. This rule contains five rules, at least two of which must be met to be classified as a drug. Lipinski's Rule of Five contains rules: molecular mass < 500 daltons; high lipophilicity (LogP < 5); molar refraction between 40-130; has < 5 hydrogen bond donors; and < 10 hydrogen bond acceptors (Lipinski, 2004).

Pharmacokinetic and Toxicity Profile Prediction

The pkCSM internet tool https://biosig.lab.uq.edu.au/pkcsm/prediction is used to predict pharmacokinetic parameters such as absorption, distribution, metabolism, and excretion, as well as the toxicity of alkaloid derivatives. The compound format entered for prediction is changed to SMILES format (Pires et al., 2015).
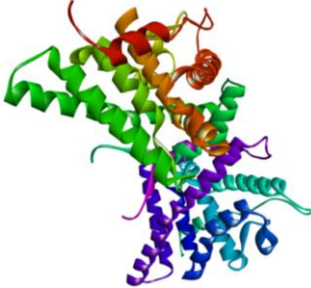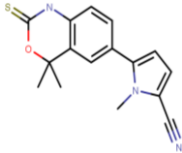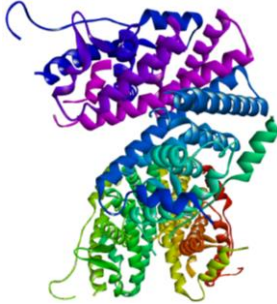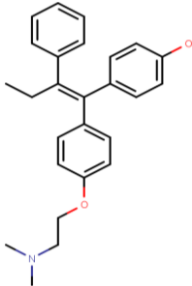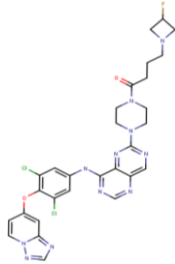
3. RESULTS AND DISCUSSION
Target Receptor Identification

Identification of target receptors is carried out to determine the quality of the protein, which can be done by analyzing several parameters, namely crystal structure resolution, Ramachandran plots, and ERRAT. Identification was carried out on three receptors in breast cancer, namely estrogen, progesterone, and HER2 receptors, each of which has PDB code 5W9C, 1ZUC, and 7PCD. The resolution of the protein crystal structure used is closely related to the quality of the protein crystals, which use X-ray diffraction crystallographic techniques to obtain protein structure information. The protein quality will be better if the protein crystal resolution value is smaller (Lu et al., 2009). Structures with resolution values of 1 Å or lower reflect a high degree of order in the crystal lattice, allowing for a substantially larger amount of diffraction data to be obtained and a finer resolution of individual atoms in the electron density map. Lower resolution electron density maps of 3 Å or better resolution can only reveal the fundamental features of the protein backbone and side chains. The overall fold and backbone structure (Cα) can be defined at low resolution (3.0 to 3.5 Å), but the unambiguous assignment of side chains is challenging (Dubach & Guskov, 2020). The resolution of each receptor is listed in **Table 1**.

Table 1. Code analysis and receptor resolution

Receptor Type	PDB	Resolution (Å)	Receptor	Ligand
Pro gesteron	1ZUC	2.00		
Estrogen	5W9C	1.80		
Tyrosine-protein kinase erbB-2 (HER2)	7PCD	1.77		

The Ramachandran plot is a diagram that illustrates the energetic position of the protein backbone through a combination of the dihedral backbone angles phi (Φ) and psi (ψ) which can also be called the torsion angle. The Ramachandran plot depicts the dihedral angles energetically permissible and prohibited zones. The distribution of observed phi (Φ) and psi (ψ) values on protein structures can be used to validate the structure. This is based on the stiffness of the N-C peptide bond, which is theoretically the permissible area of the Ramachandran plot, which shows what values of Phi/Psi angles are feasible for an amino acid, X, in a α-X-α tripeptide. It is limited by the sterically unfavorable conformation of the structure due to the linkages between the non-bonded atoms. This can happen if many dihedral angles are observed in the Ramachandran plot's limited area in a poor-quality homology model. Such variances generally suggest a structural issue (Tam et al., 2020; Wiltgen, 2018).

The Ramachandran plot is divided into four areas, namely the most favored area, the additional area that is allowed, the area that is widely allowed, and the area that is prohibited. More than 90% of the residues in a good protein structure should be in the most advantageous location. (Carugo & Djinovic Carugo, 2013). The results of the analysis of the three receptor Ramachandran plots show that the three receptors have a stable structure and good quality. This can be observed through the results of quadrant I and quadrant IV. 5W9C has the highest quadrant I value of 95.6% and the lowest is 93.0%, which is owned by 1ZUC. For quadrant IV, the highest value is owned by 7PCD with a value of 0.4%, and other receptors, namely 1ZUC and 5W9C, have the same value of 0.0%. The complete results of the Ramachandran plot can be seen in **Figure 2**. From the results of the Ramachandran plot, it can be concluded that the three identified receptors do not violate the parameters of the Ramachandran plot and can be used for the next stage.

(a)

(b)

(c)
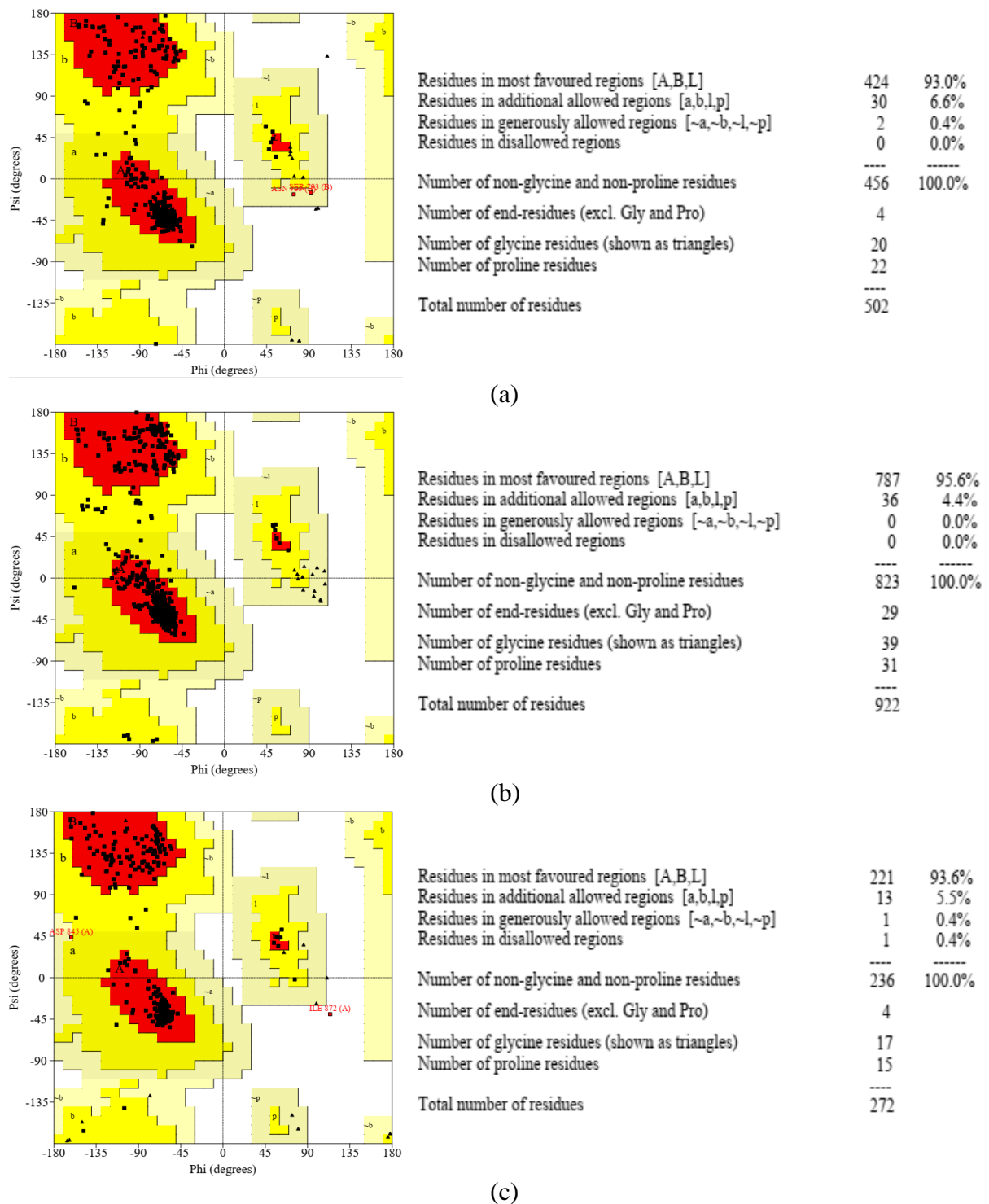
Figure 2. Ramachandran Plot of (a) 1ZUC, (b) 5W9C, and (c) 7PCD

ERRAT investigates the atomic level interactions of several amino acids. The ERRAT software (Wallner, 2006) examines the atomic level binding interactions of various amino acids. The ERRAT software examines the frequency of noncovalent interactions between distinct kinds of atoms. This is an expansion of the earlier 3D profiling method from the residue to the atomic level. Because three types of atoms (C, N, and O) are included, six forms of interactions are available (CC, CN, CO, NN, NO, and OO). The ERRAT quality factor's total value, represented as the proportion of protein whose estimated value is less than the 95% rejection level. Good high-resolution structures typically provide values of 95% or higher (Colovos & Yeates, 1993). The ERRAT values of each receptor were

99.4273%, 99.3814%, and 95.5357% for 5W9C, 1ZUC, and 7PCD, respectively. Because the three receptors have ERRAT values that exceed 95%, it can be concluded that the three receptors have high resolution and the results of the ERRAT values for each receptor can be seen in **Figure 3**.

Receptor and Ligand Preparation

For the preparation of the ligand, protonation was carried out adjusted to the blood pH, namely 7.4, and a conformation was carried out so that the ligand could be in the position with the lowest or most stable energy so that it could interact with the active site of the receptor. The conformation with the lowest energy was chosen from the 10 conformations conducted for use in the following stage. As for the preparation of the receptor, it is done to remove water molecules on the receptor so as not to interfere with the receptor-ligand interaction (Ruswanto et al., 2022).
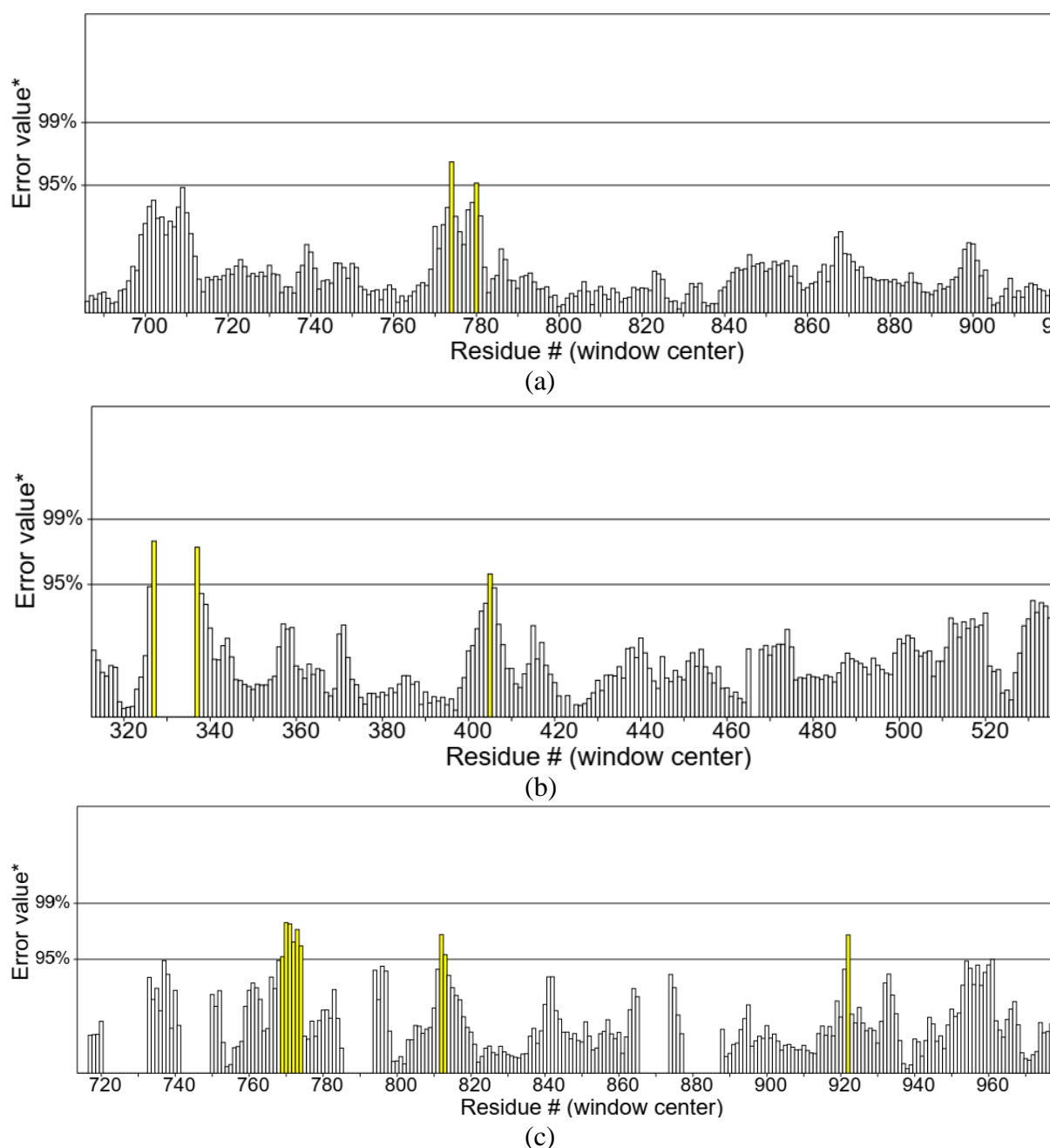
Figure 3. ERRAT result values of (a) 1ZUC, (b) 5W9C, and (c) 7PCD.

Molecular Docking Validation

The native ligand was re-docking to each active site of the receptor for molecular docking validation, which is 5-(4,4-dimethyl-2-thioxo-1,4-dihydro-2h-3,1-benzoxazin-6-yl)-   1-methyl-1h-pyrrole-2-carbonitrile (T98) against the progesterone receptor (1ZUC), 4-hydroxytamoxifen (OHT) against the estrogen receptor (5W9C), and 1-[4-[4-[[3,5-bis (chloranyl)-4-([1,2,4]triazolo[1,5-a]pyridine-7-yloxy)phenyl]amino]pyrimido[5,4-d]pyrimidin-6-yl]piperazine-1-   yl]-4-(3-fluoranylasethidine-1-yl)butan-1-one (70I) against the HER2 receptor (7PCD). **Figure 4** depicts an overlay view of the crystallographic structure and the re-docking outcomes. **Table 2** displays grid box size data for each receptor, as well as the locations and values of the re-docking outcomes.

The similarity value based on the comparison of changes in the distance and conformation of the best ligand in the outcomes of re-docking with the distance and conformation of the initial ligand is the receptor validation parameter. The result of re-docking is called valid if the RMSD value < 2 Å (Ruswanto et al., 2022). Because the RMSD of the three receptors is less than 2 Å, it may be assumed that the re-docking data are legitimate and can be utilized for docking investigations.

Molecular Docking

Virtual screening using the Autodock Vina program (Trott & Olson, 2009) is carried out for all test compounds, each of which will get 20 conformations sorted based on binding affinity values and all test compounds will also be sorted in the same way. The five test compounds for each receptor with the best binding affinity are listed in **Table 3**. Furthermore, the molecular binding process was carried out only on the best test compound with 7PCD because it has a lower binding affinity than the other two receptors.

In molecular docking, the value of binding affinity, inhibition constant and various types of bonds that occur in alkaloid compounds can be seen. Native ligands with lower energy binding affinity values are more likely to interact with proteins target. The Gibbs free energy (kcal/mol) represents the complex's state of equilibrium and stability during the protein-ligand binding process. Meanwhile, the inhibition constant value reflects the power of the drug in blocking receptor work; the lower the value, the higher the inhibition (Forli et al., 2016; Sunani et al., 2022). From the results of the binding energy of the molecule docking, it can be seen that only 7-ethylcamptothecin with a value of -7.57 kcal/mol whose value is below that of the comparator drug, namely tamoxifen with a value of -7.83 kcal/mol.

Table 2. Molecular docking validation results

Ligand	PDB	Grid Box Dimension			Grid Center			Spacing (Å)	RMSD (Å)	Binding affinity (kcal/mol)
		X	Y	Z	X	Y	Z			
T98	1ZUC	27.746	-7.72	8.992	40	40	40	0.375	0.75	-8.24
OHT	5W9C	15.044	-10.616	-26.4	40	40	40	0.375	0.68	-10.71
70I	7PCD	8.413	-8.996	-13.532	40	44	40	0.375	1.62	-8.97

(a)   (b)   (c)

Figure 4. Native ligand stack results from each receptor before (green) and after (yellow) docking (a) 1ZUC, (b) 5W9C, and (c) 7PCD

Table 3. Best virtual screening results

| PDB	No.	Compound Name	Binding Affinity (kcal/mol)
1ZUC	1.	Rutaecarpine	-10.9
	2.	Dihydrosanguinarine	-10.6
	3.	Sempervirine	-10.6
	4.	Berberrubine	-10.2
	5.	16-Epikoumidine	-10
5W9C	1.	Neolitsine	-9.7
	2.	Bicuculline	-9.3
	3.	Seneciphylline	-9.3
	4.	11-Hydroxygelsenicine	-9.1
	5.	16-Hydroxytabersonine	-9.1
7PCD	1.	Daurisoline	-11.2
	2.	Solasodine	-11.1
	3.	Sambutoxin	-10.7
	4.	7-Ethylcamptothecin	-10.6
	5.	7-Ethyl-10-Hydroxycamptothecin	-10.5

(a) (b) (c)

(d) (e)
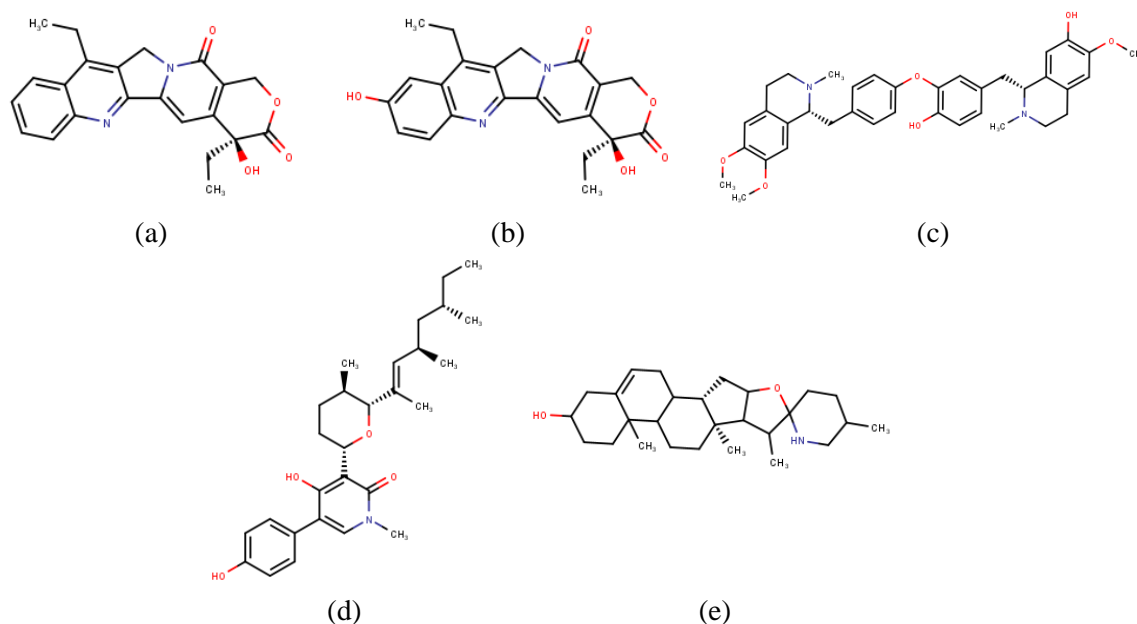
Figure 5. Chemical structure of (a) 7-Ethylcamptothecin, (b) 7-Ethyl-10-Hydroxycamptothecin, (c) Daurisoline, (d) Sambutoxin, and (e) Solasodine

Meanwhile, compared to the native ligand 7PCD (70I) with -10.03 kcal/mol, only daurisoline can give a better value of -11.48 kcal/mol. When the Gibbs free energy is lower, it indicates that the chemical-receptor interaction is more stable and that the molecule has a higher affinity for the receptor (Ruswanto et al., 2021). If the alkaloid compounds are sorted based on the lowest bond energy, then the order is daurisoline, solasodine, sambutoxin, 7-ethyl-10-hydroxycamptothecin, and 7-ethylcamptothecin with respective values of -11.48, -9.85, -8.89, -8.11, and - 7.57 kcal/mol respectively. The alkaloid compounds with inhibition constant values sorted from the smallest were daurisoline, solasodin, sambutoxin, 7-ethyl-10-hydroxycamptothecin, and 7-ethylcamptothecin each with inhibition constants of 3.82 nM, 60.45 nM, 303.79 nM, 1.14 µM, and 2.85 µM respectively. This is in line with the order of free energy values where only daurisoline has a lower value than 1.81 µM tamoxifen and 44.42 nM native ligand, and only 7-ethylcamptothecin has a constant inhibition

value under tamoxifen. This can be interpreted as only daurisoline has a more stable interaction than tamoxifen and 70I. The chemical structure of the five best compounds from HER2 virtual screening given in **Figure 5**.
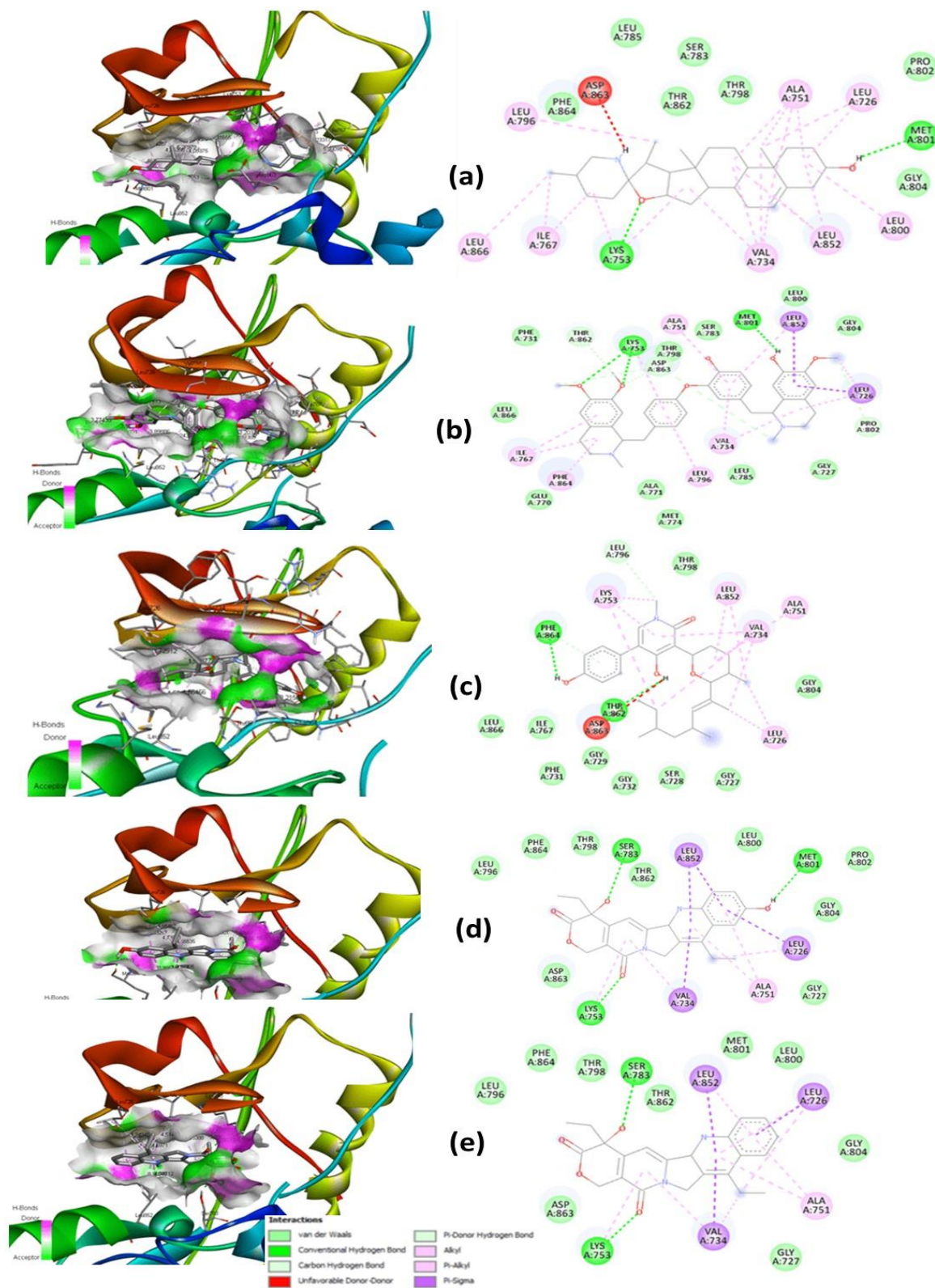
Figure 6. 3D and 2D visualization of molecular docking results of (a) Solasodine, (b) Daurisoline, (c) Sambutoxin, (d) 7-ethyl-10-hydroxycamptothecin, and (e) 7-ethylcamptothecin

The five alkaloid compounds were visualized in 3D and 2D for the interaction of ligands and amino acid residues as shown in **Figure 6**. The closer the ligand bonds are to the amino acid residues on the receptor, the more ligand bonds there are with these residues, and therefore the more durable the resultant bond. Based on the lowest free energy value and inhibition constant, daurisoline has three hydrogen bonds (LysA:753 2x, MetA:801), four hydrogen-carbon bonds (ProA:802, AspA:863 3x), and eleven van der waals bonds (GlyA: 727, LeuA:785, MetA:774, AlaA:771, GluA:770, LeuA:866, PheA:731, ThrA:798, SerA:783, LeuA:800, GlyA:804). Conventional hydrogen bonds with residues MetA:801 and LysA:753 are present in 5 and 4 compounds respectively, therefore these two residues have a possibly important role in the stability of the ligand interaction with 7PCD. Because it has the potential to affect the physicochemical characteristics and biological activities of compounds, hydrogen bonding is the preferred bond type in ligand-receptor interactions. The hydrophobic bonds that are predicted to successfully bind to the receptor show the amount of drug solubility in the cell membrane. Since the thiourea derivatives and native ligands share several groups in common, such as C=O, -NH, and a benzene ring, these compounds exhibit hydrogen bonding and are hydrophobic (Ruswanto, Mardianingrum, et al., 2022).

Daurisoline has been demonstrated in several trials to trigger cancer cell death in a variety of cancers, including esophageal squamous cell carcinoma(Wang et al., 2023), cervical HeLa (Wu et al., 2017), and bladder cancer (Huang et al., 2022). Solasodin is also reported to have anticancer effectiveness in several cancer cells such as colon, hepatocellular, lung, cervix, stomach, glioblastoma, and breast cancer (Dey et al., 2019). In addition, 7-Ethyl-10-Hydroxycamptothecin has potential as an anti-colorectal cancer (Yang et al., 2022). Sambutoxin has activity to inhibit the proliferation of several cancer cells through the mitochondrial apoptotic pathway (Li et al., 2018). Following prior research and molecular docking in this work, the five alkaloid compounds as possible breast cancer inhibitors were tested for stability using molecular dynamics simulations.

Molecular Dynamics

Based on general models of physics that drive interatomic interactions, molecular dynamics (MD) Simulations anticipate the movement of individual atoms in a protein or other molecular system over time. These simulations may disclose the locations of all atoms throughout a range of essential biomolecular events, such as conformational changes, ligand binding, and protein folding, with femtosecond temporal accuracy. (Hollingsworth & Dror, 2018). Molecular docking results are combined with molecular dynamics simulation techniques to obtain more reliable results (Mario et al., 2021). molecular dynamics simulations were performed on the substances daurisoline, solasodine, sambutoxin, 7-ethyl-10-hydroxycamptothecin, 7-ethylcamptothecin, tamoxifen and 1-[4-[4-[[3,5-bis(chloranyl)-4-([1,2,4]triazolo[1,5-a]pyridine-7-yloxy)phenyl]amino]pyrimido[5,4-d]pyrimidin-6-yl]piperazine-1-yl]-4-(3-fluoranylazetidin-1-yl)butan-1-one (70I) as a comparison. **Figure 7** depicts the MD 100 ns simulated RMSD graph of the HER2-ligand complex's stability. When the RMSD curve flattens, it indicates that the protein has stabilized and there has been a significant shift in its structure from its starting location. In **Figure 7**, all the best ligands experience fluctuations in RMSD values starting from 0 to 10 ns. However, the solasodine-HER2 complex, daurisoline-HER2, and sambutoxin-HER2 stabilized at 10 ns until the end of 100 ns. The 7-ethylcamptothecin-HER2 complex fluctuated in RMSD values up to the first 50 ns and then stabilized until the end of 100 ns.

Meanwhile, the 7-Ethyl-10-Hydroxycamptothecin-HER2 complex experienced a longer RMSD value fluctuation of up to 60 ns which then underwent stabilization until the end of 100 ns. At the conclusion of the 100 ns simulation, only the solasodine-HER2, daurisoline-HER2, and sambutoxin-HER2 complexes had RMSD curve stability close to 70I-HER2 and tamoxifen-HER2. The most stable best ligand interactions with an average RMSD occurred in the sambutoxin-HER2 complex (3,613 Å), followed by the solasodine-HER2 complex (3,899 Å), daurisoline-HER2 (4,177 Å), 7-ethylcamptothecin-HER2 (4,205 Å), and 7-ethyl-10-hydroxycamptothecin-HER2 (4,638 Å). However, when compared with the 70I-

HER2 complex (3.321 Å) and tamoxifen-HER2 (3.16 Å), all native ligands did not have a better value. This RMSD graph indicates that the complex has a steady interaction during the MD simulation. A RMSF graphical computation was performed to examine the flexibility of residues, the results of which are given in **Figure 7**.

Table 4. Result of molecular docking to the HER2 receptor (7PCD)

| Ligand | Binding Affinity (Kcal/Mol) | Inhibition Constant | Residue Interaction | | |
			Conventional Hydrogen Bonds / Distance (Å)	Hydrogen Carbon Bonds	Van Der Waals
Native ligand	-10.03	44.42 nM	LeuA:785 (2.82), MetA:801 (1.88)	LeuA:726 (2x), GlnA:799, GlyA:804	GlyA:727, SerA:728, IleA:752, MetA:774, SerA:783, ArgA:784, LeuA:796, ValA:797, ThrA:798, LeuA:800, AspA:808, ArgA:849, ThrA:862, AspA:863, PheA:864,
Tamoxifen	-7.83	1.81 µM	MetA:801 (5.32; 3.97)	MetA:801	SerA:783, LeuA:796, ValA:797, IleA:752, ThrA:862, GlnA:799, PeoA:802, LeuA:726, LeuA:800, TyrA:803, GlyA:804
7-Ethyl-10-Hydroxycamptothecin	-8.11	1.14 uM	LysA:753 (2.20), SerA:783 (1.98), MetA:801 (2.15)		GlyA:727, AspA:863, LeuA:796, PheA:864, ThrA:793, ThrA:862, LeuA:800, ProA:802, GlyA:804
7-Ethylcamptothecin	-7.57	2.85 µM	LysA:753 (2.29), SerA:783 (1.94)		GlyA:727, AspA:863, LeuA:796, PheA:864, ThrA:798, ThrA:862, MetA:801, LeuA:800, GlyA:804
Daurisoline	-11.48	3.82 nM	LysA:753 (6.54; 5.30), MetA:801 (3.62)	ProA:802, AspA:863 (3x)	GlyA:727, LeuA:785, MetA:774, AlaA:771, GluA:770, LeuA:866, PheA:731, ThrA:798, SerA:783, LeuA:800, GlyA:804
Sambutoxin	-8.89	303.79 nM	ThrA:862 (1.87), PheA:864 (1.98)	LeuA:796	GlyA:727, SerA:728, GlyA:732, GlyA729, PheA:731, IleA:767, LeuA:866, ThrA:798, GlyA:804
Solasodine	-9.85	60.45 nM	LysA:753 (4.63), MetA:801 (2.20)		PheA:864, LeuA:785, ThrA:862, SerA:783, ThrA:798, ProA:802, GlyA:804
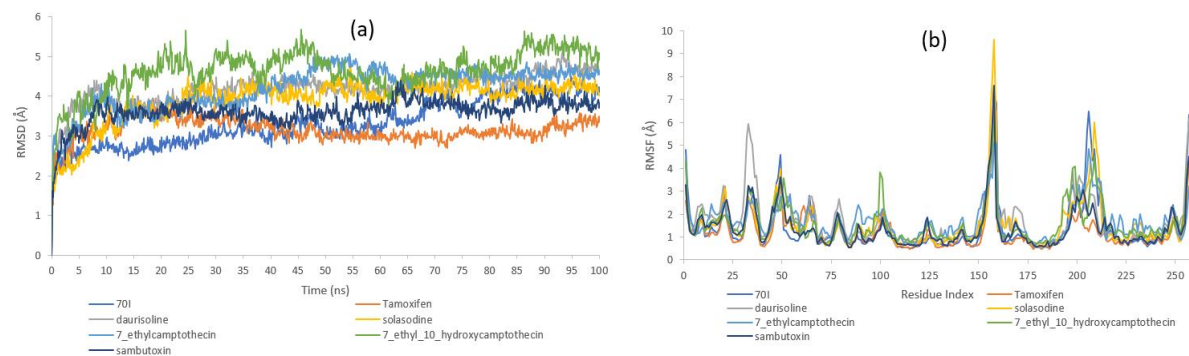
Figure 7. Combined plot of the five alkaloid compounds with comparison tamoxifen and native ligand 7PCD (70I) (a) RMSD plot of the ligand-NUDT5 complex: Tamoxifen compound (red), 7_ethyl_10hydroxycamptothecin compound (green), Solasodine (yellow), 70I (dark blue), 7-Ethylcamptothecin (light blue), and Daurisoline (gray) and (b) RMSF Plot of the system of Tamoxifen compounds, 7_ethyl_10hydroxycamptothecin compounds, Solasodine, 70I, 7-Ethylcamptothecin, and Daurisoline.
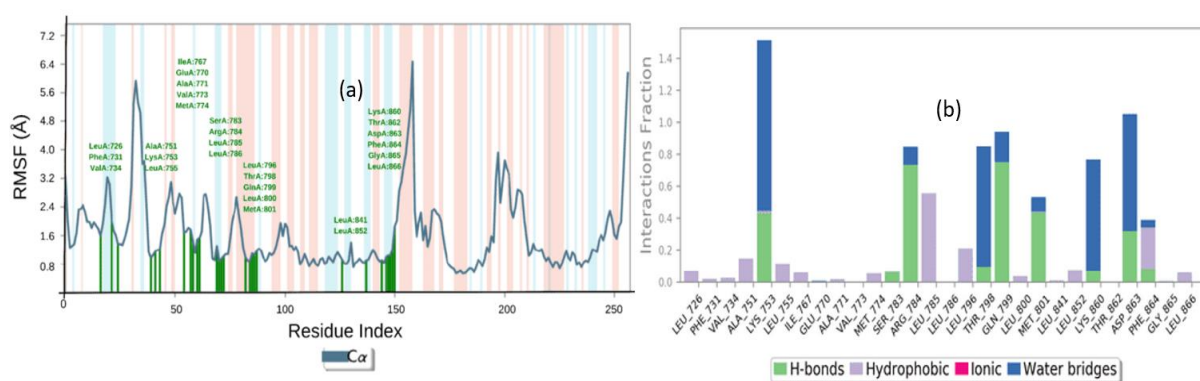
Figure 8. The results of the MD cycle of the HER2 complex are shown in (a) the RMSF graph of the residue contact and (b) Histogram of the contact residue in the 100 ns MD simulation.

Local residual flexibility was determined using RMSF (Root Mean Square Fluctuation), and RMSF ligands were evaluated for fluctuations in ligand atoms. RMSF is the average RMSD over time when dynamic system fluctuations exceed a well-defined average. It is quite convenient to determine which residues are important for the conformational change by looking at the RMSF for each carbon atom in the residue. If the RMSF of these residues fluctuates more in the simulation, it indicates that the residuals have quite a lot of flexibility (Su et al., 2022). According to the RMSF results, all the complexes have identical residual movement patterns. The protein's amino and carbon terminals are very flexible, but most of the residues are rigidly flexible. This suggests that ligand binding causes no major change in protein structure. MD simulation findings demonstrate that, in addition to RMSD and RMSF, there are changes in hydrogen and hydrophobic interactions that occur with each ligand-HER2 complex.

Figure 7 also presents RMSF plots of the complex compounds sambutoxin-HER2, solasodine-HER2, daurisoline-HER2, 7-ethylcamptothecin-HER2, and 7-Ethyl-10-Hydroxycamptothecin-HER2 as well as 70I-HER2 and tamoxifen-HER2. The residues fluctuated in the same region, with the sambutoxin-HER2 complex having the lowest variations outside of the 70I-HER2 and tamoxifen-HER2 complexes. The average RMSF values of the complex ligand compounds were sambutoxin-HER2 (1,381 Å), solasodine-HER2 (1,537 Å), daurisoline-HER2 (1,659 Å), 7-ethylcamptothecin-HER2 (1,666 Å), and 7-Ethyl-10-Hydroxycamptothecin-HER2 (1,587 Å), as well as for 70I-HER2 (1,453 Å), and tamoxifen-HER2 (1,219 Å). The protein's amino and carbon terminals are highly flexible, but the bulk of residues are rigidly flexible. This indicates that the binding of the ligand does not result in a significant conformational change of the protein. From **Figure 7** data, we can see that sambutoxin is the most stable as well as having the best interaction with HER2.

Figures 8 (a) and (b) show the 28 contact residues with the daurisoline compound. The residue interacts through several types of bonds, namely hydrogen bonds (Lys:753, Ser:783, Arg:784, Thr: 798, Gln:799, Met:801, Lys:860, Asp:863, Phe:864), hydrophobic (Leu:726, Phe:731, Val:734, Ala:751, Leu:755, Ile:767, Ala:771, Met:774, Leu:785, Leu:796, Leu:800, Leu:841, Leu:852 , Phe:864, Gly:865, Leu:866), and water bridges (Lys:753, Arg:784, Gln:799, Met:801, Lys:860, Asp:863, Phe:864).

Analyzing the contact residues of the solasodin-HER2 complex revealed 25 (Leu:726, Phe:731, Val:734, Ala:751, Lys:753, Ile:767, Ala:771, Met:774, Ser:783, Arg:784 , Leu:785, Leu:796, Thr:798, Leu¬:800, Met:801, Tyr:803, Gly:804, Cys:805, Asp:808,

Arg:849, Leu:852, Val:853, Thr:862, Asp:863, Phe:864) contact residue; for the sambutoxin-HER2 complex, 24 (Leu:726, Val:734, Phe:731, Ala:751, Lys:753, Ile:767, Glu:770, Ala:771, Ser:783, Leu:785, Met :774, Leu:796, Thr:798, Gln:799, Leu:800, Met:801, Tyr:803, Cys:805, Leu:852, Ile:861, Asp:863, Thr:862, Phe:864 , Gly:865) residues were identified.

The interactions of the residues with the ligands in each pass are shown in Figure 9(a). Some of the protein residues make numerous unique interactions with the ligands, giving the protein a richer orange hue. As shown in **Figure 9(b)**, six variables were studied to explain the stability of the cyclic acid on the HER2 receptor throughout the 100 ns MD simulation.
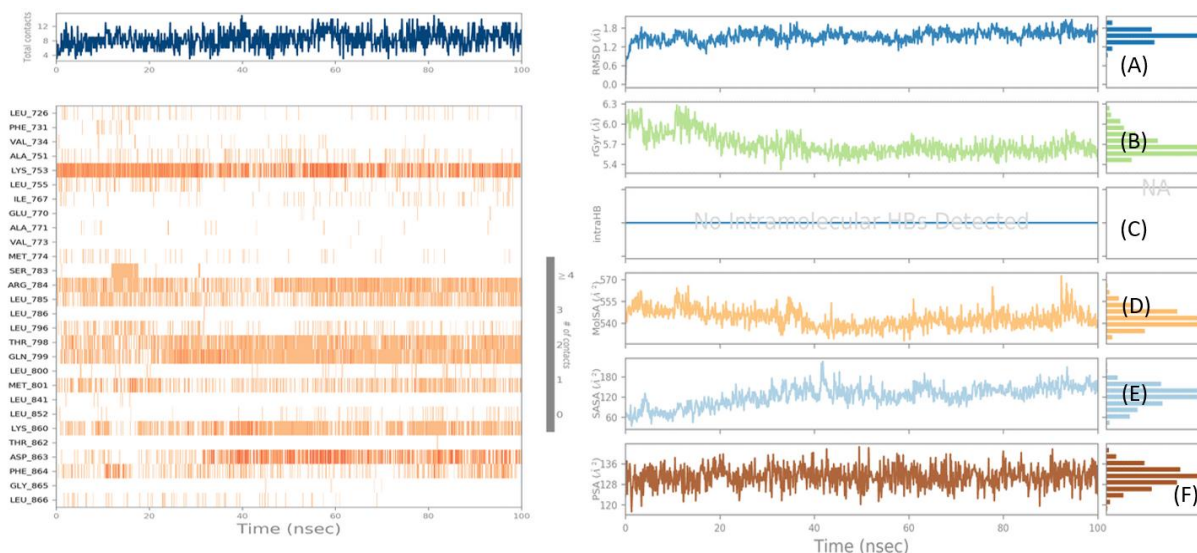
Figure 9. MD simulation results of the daurisoline-HER2 complex (left) Representation of contact residues and interactions of the daurisoline compounds during MD 100 ns and (right) Characterization of the daurisoline compounds: A. RMSD ligand, B. radius of gyration (rGyr), C. NS34, D, molecular surface area (MolSA), E. solvent accessible surface area (SASA), and F. polar surface area (PSA).
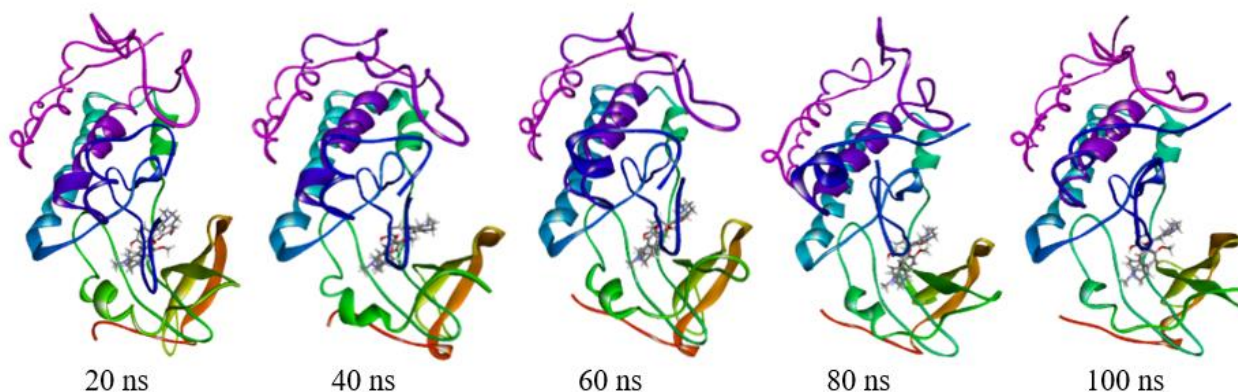
Figure 10. Changes in conformational trajectories of the daurisoline compounds in 100 ns MD simulations

Figure 9(b) depicts the fluctuating simulation method for daurisoline compounds. RMSD discovered that variations occur between 0 and 10 ns. Fluctuations occurred from 0 to 20 ns at the start of time, then stabilized until the completion of the MD simulation for the radius of gyration. The radius of the 100 ns gyration simulation ranges from 5.4 to 6.3 Å. However, the intramolar H-bond plot did not show bonding from the start of the simulation to the end. The MolSA plot shows fluctuations at the beginning (0 to 20 ns) and at the end of the simulation at 90 ns and stabilizes until the end. The SASA plot shows minimal fluctuations throughout the MD simulation time with slight fluctuations from 40 to 43 ns. PSA plots show little fluctuation and are relatively stable throughout the molecular dynamics' simulations.

The conformational changes in the daurisoline-HER2 combination occurred during the 100-ns MD simulation. However, conformational alterations in the HER2 protein's binding site persist. **Figure 10** depicts the conformational change of the HER2-ligand combination in the MD simulation findings. The time trajectory is shown for the 100 ns MD simulation with time intervals of 20, 40, 60, 80, and 100 ns.

Ligand-Based Drug Similarity Screening (Drug Scan)

Lipinski's rule of five may be used to discriminate between drug-like and non-drug-like chemicals, assisting scientists in the development of novel medications by taking into account the degree of absorption or permeability of the lipid bilayer present in the human body. Furthermore, the lipinski website was utilized to evaluate ligands based on medication similarity (Jayaram et al., 2012; Lipinski, 2004). **Table 5** presents the results. The molecular weight of compounds can affect permeability in the gastrointestinal tract and the central nervous system. This is because the greater the molecular weight of a compound, the rate of permeation in the lipid bilayer will decrease, so the ability to penetrate biological membranes decreases. In the ligands of the test compounds, only daurisoline has a molecular weight exceeding 500.

Lipophilicity describes the ability of a molecule to partition into octanol with respect to water, which correlates with the rate of absorption. The ability to dissolve in hydrophobic compounds such as oil and non-polar solvents is often expressed in the logarithmic ratio of the compound partitioned into the organic phase with the aqueous phase (Log P). The higher the Log P value, the more hydrophobic it is, and if the Log P value is > 5, the compound will be hydrophobic enough to be in the lipid bilayer for a certain time to cause toxicity (Pollastri, 2010).

The laws governing hydrogen bonding donors and acceptors correspond to the physicochemical features of the substances that form hydrogen bonds. Hydrogen bond donors are associated with a compound's biological activity, while hydrogen bond acceptors are related to permeability via interactions with strong hydrogen bonding solvents. As a result, chemicals that interact with polar solvents can lower lipid bilayer permeability. The total polarization of the drug, which is highly dependent on refractive index, pressure, and temperature, is related to the refractory molar. This polarization is affected by molecular structure and relative mass; usually, the more electrons present, the easier the polarization is to recognize. Based on the Lipinski five rules, the five compounds can be said to pass the Lipinski five rules because they fulfill at least two of the five rules, so based on the screening results, the five compounds have good drug similarity profiles.

Table 5. Best Lipinski 7PCD alkaloid compound results

Ligand	Molecular Weight	Donor Hydrogen Bond	Acceptor Hydrogen Bond	Log P	Molar Refractivity
Daurisoline	610	2	6	5.898751	173.4846
Solasodine	413	1	2	5.997142	138.18927
7-Ethylcamptothecin	376	0	5	2.271909	98.083984
Sambutoxin	453	1	4	5.464331	137.972290
7-Ethyl-10-Hydroxycamptothecin	392	1	6	1.55732	99.670792

Table 6. Best compound pharmacokinetic and toxicity profile

Property	Parameter		Dauri soline	Solaso dine	Sambu toxin	7-ethyl-10-hydroxyca mptotheci n	7-ethylca mptoth ecin
Absorption	Water Solubility (Log Mol/L)		-3.652	-3.809	-4.327	-3.318	-3.793
	Caco2 Permeability		0.567	1.292	0.913	0.366	1.115
	Intestinal Absorption (Human) (% Absorbed)		89.915	92.324	92.436	99.962	99.879
	Skin Permeability (Log Kp)		-2.735	-3.23	-2.753	-2.745	-2.743
	P-Glycopro tein	Substrate (Yes/No)	Yes	Yes	Yes	No	No
		I Inhibitor	Yes	Yes	Yes	No	Yes
		II Inhibitor	Yes	Yes	Yes	Yes	Yes
Distribution	Vdss (Human) (Log L/Kg)		-0.763	0.324	1.38	0.123	0.013
	Fraction Unbound (Human) (Fu)		0.202	0.195	0	0.108	0.211
	BBB Permeability (Log BB)		-1.047	0.035	-0.301	-0.596	-0.565
	CNS Permeability (Log PS)		-2.623	-3.047	-1.856	-3.221	-2.301
Metabolism	2D6 Substrat		Yes	No	No	No	No
	3A4 e		Yes	Yes	Yes	Yes	Yes
	CYP 1A2 (Yes/No)		No	No	No	Yes	Yes
	2C19		Yes	No	Yes	No	No
	2C9 Inhibitor		No	No	Yes	Yes	No
	2D6		Yes	No	No	No	No
	3A4		Yes	No	Yes	No	No
Excretion	Total Clearance (Log Ml/Min/Kg)		0.967	0.09	0.557	0.45	0.809
	Renaloct2 Substrate (Yes/No)		No	No	No	No	Yes
Toxicity	AMES Toxicity (Yes/No)		Yes	No	No	No	No
	Max. Tolerated Dose (Human) (Log Mg/Kg/Day)		0.255	-0.375	-0.118	-0.29	-0.198
	Herg I Inhibitor (Yes/No)		No	No	No	No	No
	Herg II Inhibitor		Yes	Yes	Yes	No	No
	Oral Rat Acute Toxicity (LD50) (Mol/Kg)		2.463	2.489	2.658	2.444	2.599
	Oral Rat Chronic Toxicity (LOAEL) (Log Mg/Kg_Bw/Day)		3.839	1.332	0.152	1.551	1.118
	Hepatotoxicity (Yes/No)		Yes	Yes	Yes	Yes	No
	Skin Sensitisation		No	No	No	No	Yes
	T.Pyriformis Toxicity (Log Ug/L)		0.285	0.311	0.519	0.302	0.323
	Minnow Toxicity (Log Mm)		-0.06	0.381	-0.844	0.691	-0.159

Pharmacokinetic and Toxicity Profile Prediction

The ADMET characteristics of the best ligand molecules displayed in **Table 6** with various parameters were identified using the pkCSM web server (Pires et al., 2015). The major components of pkCSM features, in addition to distance-based characteristics, correspond to molecular characteristics such as toxicophore fingerprints, the number of atomic pharmacophore frequencies, lipophilicity, BM, surface area, the number of bonds that may be rotated, and so on (Kar & Leszczynski, 2020). Absorption, distribution, metabolism, excretion, and toxicity must all be followed by drug-like substances (Selick et al., 2002). For the chosen ligands, blood-brain barrier (BBB), human intestinal absorption (HIA), Caco-2 cell permeability, and AMES tests were discovered. Oral medicines are largely absorbed in the intestines.

4. CONCLUSIONS

According to the results of molecular docking, the daurisoline compound has the lowest free energy with -11.48 kcal/mol and an inhibitory constant value of 3.82 nM when compared to the other four alkaloid ligands, native ligand, and tamoxifen, supported by 100 ns molecular dynamics simulations. Molecular dynamics results show that the compounds sambutoxin, solasodine, and daurisoline have RMSD, RMSF values, and stability like tamoxifen and 70I in HER2 receptor. As a

result, more study on the three compounds can be conducted to find and develop novel compounds as anti-breast cancer possibilities.

ACKNOWLEGMENTS

REFERENCES

Carugo, O., Djinovic Carugo, K. (2013). Half a century of Ramachandran plots. *Acta Crystallographica Section D: Biological Crystallography*, *69*(8), 1333–1341. https://doi.org/10.1107/S090744491301158X

Colovos, C., Yeates, T. O. (1993). Verification of protein structures: Patterns of nonbonded atomic interactions. *Protein Science*, *2*(9), 1511–1519. https://doi.org/10.1002/pro.5560020916

Devarajan, P. V., Dandekar, P., D'Souza, A. A. (2019). *Targeted Intracellular Drug Delivery by Receptor Mediated Endocytosis* (39 ed.). Springer. https://doi.org/https://doi.org/10.1007/978-3-030-29168-6

Dey, P., Kundu, A., Chakraborty, H. J., Kar, B., Choi, W. S., Lee, B. M., Bhakta, T., Atanasov, A. G., Kim, H. S. (2019). Therapeutic value of steroidal alkaloids in cancer: Current trends and future perspectives. *International Journal of Cancer*, *145*(7), 1731–1744. https://doi.org/10.1002/ijc.31965

Dubach, V. R. A., Guskov, A. (2020). The Resolution in X-ray Crystallography and Single-Particle Cryogenic Electron Microscopy. *Crystals*, *10*(580), 1–13. https://doi.org/10.3390/cryst10070580

Dutta, B., Banerjee, A., Chakraborty, P., Bandopadhyay, R. (2018). In silico studies on bacterial xylanase enzyme: Structural and functional insight. *Journal of Genetic Engineering and Biotechnology*, *16*(2), 749–756. https://doi.org/10.1016/j.jgeb.2018.05.003

Florová, P., Sklenovský, P., Banáš, P., Otyepka, M. (2010). Explicit water models affect the specific solvation and dynamics of unfolded peptides while the conformational behavior and flexibility of folded peptides remain intact. *Journal of Chemical Theory and Computation*, *6*(11), 3569–3579.

https://doi.org/10.1021/ct1003687

Forli, S., Huey, R., Pique, M. E., Sanner, M. F., Goodsell, D. S., Olson, A. J. (2016). Computational protein–ligand docking and virtual drug screening with the AutoDock suite. *nature protocols*, *11*(5), 905–919. https://doi.org/10.1038/nprot.2016.051

Halgren, T. A. (1999). MMFF VII. Characterization of MMFF94, MMFF94s, and other widely available force fields for conformational energies and for intermolecular-interaction energies and geometries. *Journal of Computational Chemistry*, *20*(7), 730–748. https://doi.org/10.1002/(SICI)1096-987X(199905)20:7<730::AID-JCC8>3.0.CO;2-T

Hollingsworth, S. A., Dror, R. O. (2018). Molecular Dynamics Simulation for All. *Neuron*, *99*(6), 1129–1143. https://doi.org/10.1016/j.neuron.2018.08.011

Huang, K., Chen, Q., Deng, L., Zou, Q., Min, S. (2022). Daurisoline Inhibiting Tumor Angiogenesis and Epithelial-Mesenchymal Transition in Bladder Cancer by Mediating HAKAI Protein Stability. *Iranian Journal of Pharmaceutical Research*, *21*(1), 1–14. https://doi.org/10.5812/ijpr-129798

Islam, M. K., Barman, A. C., Qais, N. (2020). Anti-Cancer Constituents from Plants : A Brief Review. *J. Pharm*, *19*(1), 83–96. https://doi.org/https://doi.org/10.3329/dujps.v19i1.47823

Jayaram, B., Singh, T., Mukherjee, G., Mathur, A., Shekhar, S., Shekhar, V. (2012). Sanjeevini: a freely accessible web-server for target directed lead molecule discovery. *BMC bioinformatics*, *13 Suppl 1*(Suppl 17). https://doi.org/10.1186/1471-2105-13-S17-S7

Jorgensen, W. L., Chandrasekhar, J., Madura, J. D., Impey, R. W., Klein, M. L. (1983). Comparison of simple potential functions for simulating liquid water. *The Journal of Chemical Physics*, *79*(2), 926–935. https://doi.org/10.1063/1.445869

Kar, S., Leszczynski, J. (2020). Open access in silico tools to predict the ADMET profiling of drug candidates. *Expert Opinion on Drug Discovery*, *15*(12), 1473–1487. https://doi.org/10.1080/17460441.2020.1798926

Laskowski, R. A., Hutchinson, E. G., Michie, A. D.,

Wallace, A. C., Jones, M. L., Thornton, J. M. (1997). PDBsum: A Web-based database of summaries and analyses of all PDB structures. *Trends in Biochemical Sciences*, *22*(12), 488–490. https://doi.org/10.1016/S0968-0004(97)01140-7

Laskowski, R. A., Jabłońska, J., Pravda, L., Vařeková, R. S., Thornton, J. M. (2018). PDBsum: Structural summaries of PDB entries. *Protein Science*, *27*(1), 129–134. https://doi.org/10.1002/pro.3289

Li, L.-N., Wang, L., Cheng, Y.-N., Cao, Z.-Q., Zhang, X.-K., Guo, X.-L. (2018). Discovery and Characterization of 4-Hydroxy-2-pyridone Derivative Sambutoxin as a Potent and Promising Anticancer Drug Candidate: Activity and Molecular Mechanism. *Molecular Pharmaceutics*, *15*(11), 4898–4911. https://doi.org/10.1021/acs.molpharmaceut.8b00525

Lipinski, C. A. (2004). Lead- and drug-like compounds: The rule-of-five revolution. *Drug Discovery Today: Technologies*, *1*(4), 337–341. https://doi.org/10.1016/j.ddtec.2004.11.007

Lu, H., Yin, D., Ye, Y., Luo, H., Geng, L., Li, H. (2009). *Correlation Between Protein Sequence Similarity and X-Ray Diffraction Quality in the Protein Data Bank*. 50–55.

Mardianingrum, R., Endah, S. R. N., Suhardiana, E., Ruswanto, R., Siswandono, S. (2021). Docking and molecular dynamic study of isoniazid derivatives as anti-tuberculosis drug candidate. *Chemical Data Collections*, *32*, 100647. https://doi.org/10.1016/j.cdc.2021.100647

Mario, D., Lobo, F., Amesty, Á., Vald, C., Canerina-amaro, A., Mesa-herrera, F., Soler, K., Boto, A., Mar, R., Est, A., Lahoz, F. (2021). *FLTX2 : A Novel Tamoxifen Derivative Endowed with Antiestrogenic , Fluorescent , and Photosensitizer Properties*.

Maximov, P. Y., Abderrahman, B., Fanning, S. W., Sengupta, S., Fan, P., Curpan, R. F., Rincon, D. M. Q., Greenland, J. A., Rajan, S. S., Greene, G. L., Jordan, V. C. (2018). Endoxifen, 4-Hydroxytamoxifen and an Estrogenic Derivative Modulate Estrogen Receptor Complex Mediated Apoptosis in Breast Cancer. *Molecular Pharmacology*, *94*(2), 812–822. https://doi.org/10.1124/mol.117.111385

Pires, D. E. V., Blundell, T. L., Ascher, D. B. (2015). pkCSM: Predicting small-molecule pharmacokinetic and toxicity properties using graph-based signatures. *Journal of Medicinal Chemistry*, *58*(9), 4066–4072. https://doi.org/10.1021/acs.jmedchem.5b00104

Pollastri, M. P. (2010). Overview on the rule of five. *Current Protocols in Pharmacology*, *SUPPL. 49*, 1–8. https://doi.org/10.1002/0471141755.ph0912s49

Qing, Z.-X., Huang, J.-L., Yang, X.-Y., Liu, J.-H., Cao, H.-L., Xiang, F., Cheng, P., Zeng, J.-G. (2017). Anticancer and Reversing Multidrug Resistance Activities of Natural Isoquinoline Alkaloids and their Structure-activity Relationship. *Current Medicinal Chemistry*, *25*(38), 5088–5114. https://doi.org/10.2174/0929867324666617092 0125135

Rampogu, S., Balasubramaniyam, T., Lee, J. (2022). Biomedicine & Pharmacotherapy Phytotherapeutic applications of alkaloids in treating breast cancer. *Biomedicine & Pharmacotherapy*, *155*(September), 113760. https://doi.org/10.1016/j.biopha.2022.113760

Raval, K., Ganatra, T. (2022). *Basics , types and applications of molecular docking : A review Basics , types and applications of molecular docking : A review*. *March*. https://doi.org/10.18231/j.ijcaap.2022.003

Research, D. E. S. (2019). *Desmond Molecular Dynamics System* (No. 2019–2). Maestro-Desmond Interoperability Tools, Schrödinger.

Ruswanto, Aprillia, A. Y., Hapid, P. A. (2022). *Monograf Telaah Analisis Bioinformatika Turunan Alkaloid Sebagai Kandidat Terapi SARS-CoV-2*. Global Aksara Pers.

Ruswanto, R., Mardianingrum, R., Yanuar, A. (2022). Computational Studies of Thiourea Derivatives as Anticancer Candidates through Inhibition of Sirtuin-1 (SIRT1). *Jurnal Kimia Sains dan Aplikasi*, *25*(3), 87–96. https://doi.org/10.14710/jksa.25.3.87-96

Ruswanto, R., Miftah, A. M., Tjahjono, D. H., Siswandono. (2021). In silico study of 1-benzoyl-3-methylthiourea derivatives activity as epidermal growth factor receptor (EGFR) tyrosine kinase inhibitor candidates. *Chemical Data Collections*, *34*(36), 100741. https://doi.org/10.1016/j.cdc.2021.100741

Selick, H. E., Beresford, A. P., Tarbit, M. H. (2002). The emerging importance of predictive ADME simulation in drug discovery. *Drug Discovery Today*, *7*(2), 109–116. https://doi.org/10.1016/S1359-6446(01)02100-6

Su, J., Sun, T., Wang, Y., Shen, Y. (2022). Conformational Dynamics of Glucagon-like Peptide-2 with Different Electric Field. *Polymers*, *14*(2722). https://doi.org/https://doi.org/10.3390/polym14132722

Sunani, Andani, M., Kamaludin, A., Stannia, N., Helmi, P., Mei, K., Guspira, Y., Sabetta, O., Aulifa, D. (2022). In Silico Study of Compounds in Bawang Dayak (Eleutherine palmifolia (L) Merr .) Bulbs on Alpha Estrogen Receptors. *Indonesian Journal of Cancer Chemoprevention*, *June*, 83–93.

Sung, H., Ferlay, J., Siegel, R. L., Laversanne, M., Soerjomataram, I., Jemal, A., Bray, F. (2021). Global Cancer Statistics 2020: GLOBOCAN Estimates of Incidence and Mortality Worldwide for 36 Cancers in 185 Countries. *CA: A Cancer Journal for Clinicians*, *71*(3), 209–249. https://doi.org/10.3322/caac.21660

Tam, B., Sinha, S., Wang, S. M. (2020). Combining Ramachandran plot and molecular dynamics simulation for structural-based variant classification: Using TP53 variants as model. *Computational and Structural Biotechnology Journal*, *18*, 4033–4039. https://doi.org/10.1016/j.csbj.2020.11.041

Tilaoui, M., Ait Mouse, H., Zyad, A. (2021). Update and New Insights on Future Cancer Drug Candidates From Plant-Based Alkaloids. *Frontiers in Pharmacology*, *12*(December), 1–19. https://doi.org/10.3389/fphar.2021.719694

Tran, N. T., Jakovlić, I., Wang, W.-M. (2015). In silico characterisation, homology modelling and structure-based functional annotation of blunt snout bream (Megalobrama amblycephala) Hsp70 and Hsc70 proteins. *Journal of Animal Science and Technology*, *57*(1), 1–9. https://doi.org/10.1186/s40781-015-0077-x

Trott, O., Olson, A. J. (2009). AutoDock Vina: Improving the Speed and Accuracy of Docking with a New Scoring Function, Efficient Optimization, and Multithreading. *Journal of computational chemistry*, *31*(2), 174–182. https://doi.org/10.1002/jcc.21334

Wallner, B. (2006). Identification of correct regions in protein models using structural, alignment, and consensus information. *Protein Science*, *15*(4), 900–913. https://doi.org/10.1110/ps.051799606

Wang, D., Zhang, W., Zhang, X., Li, M., Wu, Q., Li, X., Zhao, L., Yuan, Q., Yu, Y., Lu, J., Zhao, J., Dong, Z., Liu, K., Jiang, Y. (2023). Daurisoline suppresses esophageal squamous cell carcinoma growth in vitro and in vivo by targeting MEK1/2 kinase. *Molecular Carcinogenesis*, *December 2022*. https://doi.org/10.1002/mc.23503

Wilding, B., Scharn, D., Böse, D., Baum, A., Santoro, V., Chetta, P., Schnitzer, R., Botesteanu, D. A., Reiser, C., Kornigg, S., Knesl, P., Hörmann, A., Köferle, A., Corcokovic, M., Lieb, S., Scholz, G., Bruchhaus, J., Spina, M., Balla, J., … Neumüller, R. A. (2022). Discovery of potent and selective HER2 inhibitors with efficacy against HER2 exon 20 insertion-driven tumors, which preserve wild-type EGFR signaling. *Nature Cancer*, *3*(7), 821–836. https://doi.org/10.1038/s43018-022-00412-y

Wiltgen, M. (2018). Algorithms for structure comparison and analysis: Homology modelling of proteins. In *Encyclopedia of Bioinformatics and Computational Biology: ABC of Bioinformatics* (Vol. 1–3). Elsevier Ltd. https://doi.org/10.1016/B978-0-12-809633-8.20484-6

Wu, M. Y., Wang, S. F., Cai, C. Z., Tan, J. Q., Li, M., Lu, J. J., Chen, X. P., Wang, Y. T., Zheng, W., Lu, J. H. (2017). Natural autophagy blockers, dauricine (DAC) and daurisoline (DAS), sensitize cancer cells to camptothecin-induced toxicity. *Oncotarget*, *8*(44), 77673–77684. https://doi.org/10.18632/oncotarget.20767

Yang, C., Xia, A. J., Du, C. H., Hu, M. X., Gong, Y. L., Tian, R., Jiang, X., Xie, Y. M. (2022). Discovery of highly potent and selective 7-ethyl-10-hydroxycamptothecin-glucose conjugates as potential anti-colorectal cancer agents. *Frontiers in Pharmacology*, *13*(November), 1–12. https://doi.org/10.3389/fphar.2022.1014854

Zhang, Z., Olland, A. M., Zhu, Y., Cohen, J., Berrodin, T., Chippari, S., Appavu, C., Li, S., Wilhem, J., Chopra, R., Fensome, A., Zhang, P., Wrobel, J., Unwalla, R. J., Lyttle, C. R., Winneker, R. C. (2005). Molecular and pharmacological properties of a potent and

selective novel nonsteroidal progesterone receptor agonist tanaproget. *The Journal of Biological Chemistry*, *280*(31), 28468–28475.

https://doi.org/10.1074/jbc.M504144200